A Model-Adaptive Clustering-Based Time Aggregation Method for Low-Carbon Energy System Optimization

Yuheng Zhang, *Student Member, IEEE*, Vivian Cheng, Dharik S. Mallapragada, Jie Song, *Senior Member, IEEE*, and Guannan He, *Member, IEEE*

***Abstract*—Intermittent renewable energy resources like wind and solar introduce uncertainty across multiple time scales, from minutes to years, on the design and operation of power systems. Energy system optimization models have been developed to find the least-cost solution that manages the multi-timescale variability using an optimal portfolio of flexible resources. However, input data that capture such multi-timescale uncertainty are characterized with a long time horizon and high resolution, which brings great difficulty to solving the optimization model. Here we propose a model-adaptive time aggregation method based on clustering to alleviate the computational complexity, in which the energy system is solved over selected representative time periods instead of the full time horizon. The proposed clustering method is adaptive to various energy system optimization models or settings, because it extracts features from the optimization models to inform the clustering process. Results show that the proposed adaptive method can significantly lower the error in approximating the solution of the optimization model with the full time horizon, compared to traditional time aggregation methods.**

***Index Terms*—Energy system optimization, time aggregation, model adaptive, intermittent renewable energy, energy storage.**

NOMENCLATURE

Indices and Sets

i, I	Index and set of renewable energy resources.
s, S	Index and set of storage.
j, J	Index and set of thermal generation.
t, τ	Index of time intervals.
T	Set of time intervals.

Parameters

c_s^{DEG}	Unit operation cost for storage s to charge and discharge (\$/MW)
c_j^{OP}	Unit operation cost for thermal plant of type j (\$/MW)
c_j^{UpDn}	Unit operation cost for each action of thermal start-up and shut-down of type j (\$)
$c_s^{\text{ENE, INV}}$	Investment cost for storage energy capacity of type s (\$/MW)
$c_s^{\text{POW, INV}}$	Investment cost for storage power capacity of type s (\$/MW)
$c_i^{\text{IRE, INV}}$	Investment cost for intermittent renewable energy capacity of resource i (\$/MW)
$c_j^{\text{THE, INV}}$	Investment cost for thermal capacity of type j (\$/MW)
L_t	Demand at time t (MW)
ξ_{min}	Minimum output percentage of thermal generation units.
ξ_{max}	Maximum output percentage of thermal generation units.
$A_{i,t}$	Generation profile of intermittent renewable resource i at time t
η	Efficiency of storage charging and discharging.
R	Total percentage of renewable energy in demand.

Variables

$x_{s,t}^{\text{DIS}}$	Amount of discharged electricity from storage system s at time t (MW)
$x_{s,t}^{\text{CHA}}$	Amount of charged electricity to storage system s at time t (MW)
$x_{j,t}^{\text{THE}}$	Amount of electricity generated from thermal type j at time t (MW)
y_s^{ENE}	Capacity of storage energy of system s (MWh)
y_s^{POW}	Capacity of storage power of system s (MW)
y_i^{IRE}	Capacity of intermittent renewable energy of resource i (MW)
y_j^{THE}	Capacity of thermal plant of type j (MW)
$n_{j,t}$	Number of online thermal generation unit of type j at time t
$n_{j,t}^{\text{UP}}$	Number of start-up thermal generation unit of type j at time t

Manuscript received 7 January 2022; revised 15 April 2022 and 11 June 2022; accepted 7 July 2022. Date of publication 17 August 2022; date of current version 19 December 2022. This work was supported by High-performance Computing Platform of Peking University. The work of Vivian Cheng was supported by the MIT Energy Initiative undergraduate research opportunities program. The work of Dharik S. Mallapragada was supported by Future Energy Systems Center at the MIT Energy Initiative. Paper no. TSTE-00020-2022. *(Corresponding author: Guannan He.)*

Yuheng Zhang is with the Department of Industrial Engineering and Management, College of Engineering, Peking University, Beijing 100871, China.

Vivian Cheng is with the Department of Civil and Environmental Engineering, Massachusetts Institute of Technology, Cambridge, MA 02139 USA.

Dharik S. Mallapragada is with the MIT Energy Initiative, Massachusetts Institute of Technology, Cambridge, MA 02139 USA.

Jie Song and Guannan He are with the Department of Industrial Engineering and Management, College of Engineering, Peking University, Beijing 100871, China, and also with the MIT Energy Initiative, Massachusetts Institute of Technology, Cambridge, MA 02139 USA (e-mail: gnhe@pku.edu.cn).

Color versions of one or more figures in this article are available at https://doi.org/10.1109/TSTE.2022.3199571.

Digital Object Identifier 10.1109/TSTE.2022.3199571

$n_{j,t}^{\mathrm{DN}}$ Number of shut-down thermal generation unit of type j at time t
N_j Total number of thermal plant of type j
w_t Amount of renewable resource curtailment at time t (MW)
$E_{s,t}$ Energy storage level of storage system s at time t (MWh)

I. Introduction

IN ORDER to keep the 1.5 °C target of the Paris Agreement in reach, human beings have to act immediately and more concretely on decarbonization according to IPCC report [1]. Countries over the world have set many targets of energy transition to lower carbon emissions. For example, in the Energy Roadmap 2050, the European Union (EU) commits itself to reducing greenhouse gas (GHG) emissions to 80-95% below 1990 levels and realizing carbon neutrality by 2050 [2]. China has announced its aims to reach peak carbon emissions before 2030 and carbon neutrality by 2060. To fulfill the targets, the share of fossil sources in China's energy sector needs to be reduced to less than 20% [3]. The USA has committed itself to the target of reducing carbon emissions to half by 2030, compared to 2005 levels, and achieving net zero emissions no later than 2050. Before the official announcement came out [4], California state had focused on direct air carbon capture [5] and intended to reach carbon neutrality by 2045 [6].

Intermittent renewable energy (IRE) resources are getting more and more deployed worldwide due to their sustainability and potential to meet energy demands with zero or near zero emissions of both air pollutants and GHGs [7]. According to the International Energy Agency, IRE resources in 2020 supplied 28% of the total world energy demand [8], reaching a 45% increase in global capacity growth, and this share is expected to increase very significantly (30–80% in 2100) [9]. However, the energy generation from IRE is variable and uncertain, in contrast to conventional thermal generation [10]. There is not only hourly variability, but also weekly, seasonal, and yearly variability in IRE generation, as shown in Fig. 1. With such variability and uncertainty, when the IRE rapidly penetrates into power grids, many grid integration problems could arise including curtailment [11] and over-generation [12].

To cope with the challenges, greater investments in flexibility resources like energy storage technologies are necessary. Energy storage can provide multiple values to energy systems, such as accommodating increased penetrations of IRE [13], load leveling and peak shaving [14], frequency regulation [15], damping energy oscillations [16], and improving power quality and reliability [17]. The global energy storage capacity is expected to triple to 181-421 GWh by 2030 [18]. To optimally match flexibility to variability in energy systems, energy system optimization models (ESOMs) are commonly used, which determine the least-cost sizes and scheduling of generation resources such as IRE, energy storage, and thermal power plants. When involved with integer variables to denote the status of thermal generation units or the decision of transmission line expansion, these models are in the form of mixed integer linear programming (MILP) [19], [20], [21], [22]. In order to capture the multi-timescale balance of variability and flexibility in future energy systems, incorporating long-term data of operation from IRE and storage systems is necessary, especially if multi-stage decarbonization policies/pathways towards the mid of the century need to be modeled. Such models are also called capacity expansion [23] problems, whose focus is on how to optimally invest new power and storage capacities for future energy supply requirements.

For long-term ESOMs in the form of MILP, the computational complexity increases dramatically as the time horizon expands. Time aggregation [24] or temporal clustering [25] techniques have been applied to reduce the complexity of these models in such situations. The main concept is to represent the full time horizon with some representative time slices, selected through finding patterns or clusters of similar supply and demand in the full time series. Many time slicing/aggregation methods have been developed. Following Haydt et al. [26] and Poncelet [27], two commonly used methods are referred to as the integral method and the semi-dynamic method. In the integral method, typically 5-10 time slices are used to distinguish between different load levels across the time horizon and each time slice represents an average load level during a certain fraction of the full horizon [26]. The semi-dynamic method is the most used time slicing method [28], [29], which disaggregates time horizon into different seasons, days of the week and diurnal periods under the assumption that the time series data change on the basis of seasonal, weekly and daily frequency. More advanced methods are in the clustering family. Nahmmacher et al. [30] used a hierarchical algorithm with ward linkage to perform clustering on the LIMES-EU model and showed that a small number of representative days developed in this way are sufficient to reflect the characteristic fluctuations of the input data. Zatti et al. [31] proposed a MILP clustering model, named k-MILP, devised to find at the same time the most representative days of the year and the extreme days. Vitali et al. [32] proposed a clustering method considering temporal correlation as an important feature in time aggregation to offer better representation in capacity expansion problems including storage and renewable energy sources, which keeps chronology in time series.

Due to the smoothing effect in clustering, extreme events including high demand and low VRE availability are typically removed, which are important for robust energy system designs [33], [34]. Authors of [33] proposed a framework by adding extreme periods manually and clustering on the remaining periods to avoid the smoothing effect. Authors of [34] pointed out that the addition of extreme periods serves two purposes: to ensure that operating constraints are met by the designed system and to improve the accuracy of the objective function value of the optimization problem.

Beyond the removal of extreme periods, some researchers have noticed that clustering on the raw data including load and generation profiles is not enough to find the optimal system design and may fail to satisfy generation reliability [35], [36]. Authors of [35] used investment costs as features, obtained by running a planning model on each individual day, and concluded that when the number of clustering is set to 50, the results of

the planning model defined on a single year could be properly approximated. Hilbers et al. [36] proposed a concept called importance subsampling following the same logic with the variable costs as new features. They firstly assigned each day with an importance index by running model on individual days and extracted the variable costs as criteria for later clustering. These studies use cost-oriented features to improve the clustering algorithm of time aggregation. However, using cost terms as features are insufficient to capture characteristics of all components in the model, which may be improved by using more features like capacities, and existing studies typically use a single day as period which is not enough for seasonal/long-duration storage planning.

Some studies [37], [38] proposed to minimize the errors of reconstructing duration curves of renewable availability and demand profiles to find representative periods and corresponding weights. While this method provides a valuable pathway, having a similar annual duration curve may not guarantee accurate modelling of long-duration storage, which requires chronological information. Moreover, such approach is beyond the scope of clustering-based time aggregation methods, which is the focus of our paper.

The traditional time aggregation methods mentioned before perform clustering based on the similarity information of the time series input data only. However, it is neglected in the studies that whether similar data profiles have similar impacts on the ESOM results, as the ESOM is usually a non-linear mapping from inputs to solutions. Taking energy systems with high share of renewable energy resources for example, the representative time series obtained by clustering input data are fixed for different penetrations of renewable energy, as the similarity of input data could not reflect the characteristics of a specific ESOM like a high or low share of renewable energy. Therefore, traditional time aggregation methods based on the similarity of raw data only may not guarantee high approximation performance for long-term ESOMs. Though there are a few articles trying to perform clustering on new feature space transformed through the mapping of model, they used cost terms as indicators of how hard to satisfy the demand [36] which is not general for optimization model on longer time horizon according to our results.

To further explore the potential of utilizing model information in time aggregation, here we propose a model-adaptive clustering-based method that combines model characteristics and input data variations in representative time period selection. Features used in clustering are decision variables extracted from processing the raw input data with an ESOM and contain similarity information from the perspective of the ESOM. For different ESOMs or policy settings, this method can adaptively select representative time periods, which can then be used to approximate the full time horizon and reduce computational complexity with lower approximation errors than traditional methods. The main contributions are three-fold: 1) we propose a more general method to extract features through dimension reduction using the ESOM as a mapping function for representative time period selection; 2) we find the best clustering configurations for the proposed model-adaptive time aggregation method; 3) we show how the proposed method is adaptive to different policy settings, which explains why the approximation errors of the proposed method are lower than traditional methods.

The remainder of this article is organized as follows: Section II describes and establishes a case ESOM including thermal generation and renewable energy resources as well as storage systems. Section III explains in detail how to implement our proposed adaptive time aggregation method. Numeric results are presented in Section IV. Section V draws conclusions.

II. Energy System Optimization Model

Bottom-up, long-term energy system planning models or capacity expansion models (CEMs) are frequently used to analyze pathways for the transition of the energy/electrical power system and to inform policy design [39]. Without loss of generality, we design a case ESOM that contains different technologies including thermal, wind, and solar generators as well as energy storage systems, to compare the performance of different time aggregation methods and validate our proposed method.

A. Objective Function

The objective function consists of variable costs in operation and fixed costs in investment denoted by C^{VAR} and C^{FIX}, as in equation (1). The decision variables are the capacities and operational schedules of each technology. For many storage technologies, the power (conversion capability) and energy (storage volume) capacities can be designed independently, denoted by y_s^{POW} and y_s^{ENE}, respectively.

$$OB = C^{\mathrm{VAR}} + C^{\mathrm{FIX}} \tag{1}$$

$$C^{\mathrm{VAR}} = C^{\mathrm{DEG}} + C^{\mathrm{OP}} + C^{\mathrm{UpDn}} \tag{2}$$

$$C^{\mathrm{DEG}} = \sum_{t\in\mathbb{T}}\sum_{s\in\mathbb{S}}(x_{s,t}^{\mathrm{DIS}} + x_{s,t}^{\mathrm{CHA}})c_s^{\mathrm{DEG}} \tag{3}$$

$$C^{\mathrm{OP}} = \sum_{t\in\mathbb{T}}\sum_{j\in\mathbb{J}} x_{j,t}^{\mathrm{THE}} c_j^{\mathrm{OP}} \tag{4}$$

$$C^{\mathrm{UpDn}} = \sum_{t\in\mathbb{T}}\sum_{j\in\mathbb{J}}(n_{j,t}^{\mathrm{UP}} + n_{j,t}^{\mathrm{DN}})c_j^{\mathrm{UpDn}} \tag{5}$$

$$C^{\mathrm{FIX}} = \sum_{s\in\mathbb{S}}(y_s^{\mathrm{ENE}} c_s^{\mathrm{ENE,INV}} + y_s^{\mathrm{POW}} c_s^{\mathrm{POW,INV}}) + \sum_{i\in\mathbb{I}} y_i^{\mathrm{IRE}} c_i^{\mathrm{IRE},v} + \sum_{j\in\mathbb{J}} y_j^{\mathrm{THE}} c_j^{\mathrm{THE,INV}} \mathrm{N}_j \tag{6}$$

Variable costs are mainly from discharge and charge actions in the storage systems, denoted by C^{DEG}, and thermal operation, which consists of two parts: operation cost and startup and shutdown costs, which are denoted by C^{OP} and C^{UpDn}, respectively. Fixed costs consist of investment costs from different technologies considered in system including energy capacity, power capacity for storage system, multi renewable capacity and thermal capacity, as in equation (2).

B. Energy Balance

For each IRE resource considered in the model, the capacity y_i^{IRE} indicates its maximum possible generation, and its profile is represented by $A_{i,t}$. When an IRE resource is over-abundant, curtailment might be needed and represented by w_t. Considering all energy inflow and outflow, the energy balance can be modelled as:

$$\sum_{i\in\mathbb{I}} y_i^{\text{IRE}} A_{i,t} - w_t + \sum_{j\in\mathbb{J}} x_{j,t}^{\text{THE}} + \sum_{s\in\mathbb{S}} \left(x_{s,t}^{\text{DIS}} - x_{s,t}^{\text{CHA}}\right) = \text{L}_t \tag{7}$$

In equation (7), $y_i^{\text{IRE}} A_{i,t}$ represents the output of IRE resource i at time t in the form of capacity multiplied by its generation profile; $x_{j,t}^{\text{THE}}$ denotes the output of thermal generator j at time t; $x_{s,t}^{\text{DIS}}$ and $x_{s,t}^{\text{CHA}}$ stand for discharged and charged energy from storage systems at time t, respectively; w_t denotes the amount of IRE curtailment; and L_t denotes power demand at time t. Each term of equation (7) should be positive.

C. Thermal Generation

The minimum and maximum generation requirements of thermal power plants when they are online are modelled as:

$$\xi_{min} y_{j,t}^{\text{THE}} \le x_{j,t}^{\text{THE}} \le \xi_{max} y_{j,t}^{\text{THE}} \tag{8}$$

where ξ_{min} and ξ_{max} denote the minimum and maximum output, respectively, as percentages of the full capacity $y_{j,t}^{\text{THE}}$. The full capacity of thermal generators is defined by the number multiplied with capacity size, which means $y_{j,t}^{\text{THE}} = n_{j,t} * capacity\ \ size$. $n_{j,t}$ denotes the number of online units. The unit commitment of thermal generators are modelled as [39]:

$$n_{j,t} - n_{j,t-1} = n_{j,t}^{\text{UP}} - n_{j,t}^{\text{DN}} \tag{9}$$

Here we did an approximation of using integer instead of binary variables for unit commitment modelling. Previous research shows that it results in a relatively small error in the overall dispatch and objective function while leading to large reductions in computational time [40].

$$0 \le n_{j,t}, n_{j,t}^{\text{UP}}, n_{j,t}^{\text{DN}} \le N_j \tag{10}$$

$$n_{j,t}, n_{j,t}^{\text{UP}}, n_{j,t}^{\text{DN}}, N_j \in \mathbb{N} \tag{11}$$

Namely the superscripts 'UP' and 'DN' denote the start-up and shut-down actions of thermal generation units, respectively. The minimum up/down time constraints respectively require units to remain online/offline for a minimum period of time after starting up/shutting down. These constraints are formulated as (9)–(13), where the minimum up and down time are denoted by t^{UP} and t^{DN}.

$$n_{j,t} \ge \sum_{\tau=t-t^{\text{UP}}}^{t} n_{j,\tau}^{\text{UP}} \tag{12}$$

$$N_j - n_{j,t} \ge \sum_{\tau=t-t^{\text{DN}}}^{t} n_{j,\tau}^{\text{DN}} \tag{13}$$

D. Storage System

The state of charge and operational limit constraints for energy storage systems are modelled as:

$$E_{s,t} - E_{s,t-1} = x_{s,t}^{\text{CHA}}\eta - \frac{x_{s,t}^{\text{DIS}}}{\eta} \tag{14}$$

$$0 \le E_{s,t} \le y_s^{\text{ENE}} \tag{15}$$

$$0 \le x_{s,t}^{\text{DIS}}, x_{s,t}^{\text{CHA}} \le y_s^{\text{POW}} \tag{16}$$

$E_{s,t}$ is the energy level at time slot t in the storage system for each type of storage device. η is efficiency of battery charging and discharging. $x_{s,t}^{\text{CHA}}$ and $x_{s,t}^{\text{DIS}}$ are the amount of electricity charged and discharged from storage device s. Storage energy level can't exceed its capacity and charging power can't overshoot power capacity.

We model renewable portfolio standards, which are very common energy policies over the world, setting lower bounds for energy supplied by renewable energy and equivalently upper bounds for fossil fuel based generation as:

$$\sum_{t=1}^{T} x_{j,t}^{\text{THE}} \le (1-\text{R}) \sum_{t=1}^{T} \text{L}_t \tag{17}$$

This R parameter controls the portfolio of dispatchable thermal generation and IRE along with the storage system. A bigger R requires a larger share of IRE and storage systems.

III. Model-Adaptive time Aggregation Method

As introduced before, there is multi-timescale variability in IRE generation, from minutes to years, and thus, solving ESOMs across a long time horizon is needed to design an energy system with high penetrations of IRE.

In long-term ESOMs, input data including IRE sources and demand profiles span across a long time horizon. Such ESOMs have extremely high dimensions, and computational intractability is a significant issue when directly solving the models [41], as in Fig. 2(a). Time aggregation is used to address the intractability through approximation.

In traditional time aggregation, as in Fig. 2(b), the full time horizon is first divided into smaller time slices in the resolution of day or week according to planning horizon. Then, clustering algorithms like k-means or hierarchical methods are applied to the time slices to group similar slices into clusters based on predefined distances between time slices, and one slice is selected to represent all slices in a cluster, typically the centroid value will be used. Solving the ESOM over the selected time slices could save computational time significantly.

Unlike traditional time aggregation in which raw data of IRE and demand profiles are used as clustering features, our proposed model-adaptive method extracts features from ESOMs for clustering, and thus, the clustering results contain model information, as shown in Fig. 2(c). The detailed procedures are as follows:

1) Choose an appropriate period length, which usually is a day or week, and split the full planning horizon T into a set of such smaller periods denoted by $T'_1, T'_2, \ldots, T'_m$;

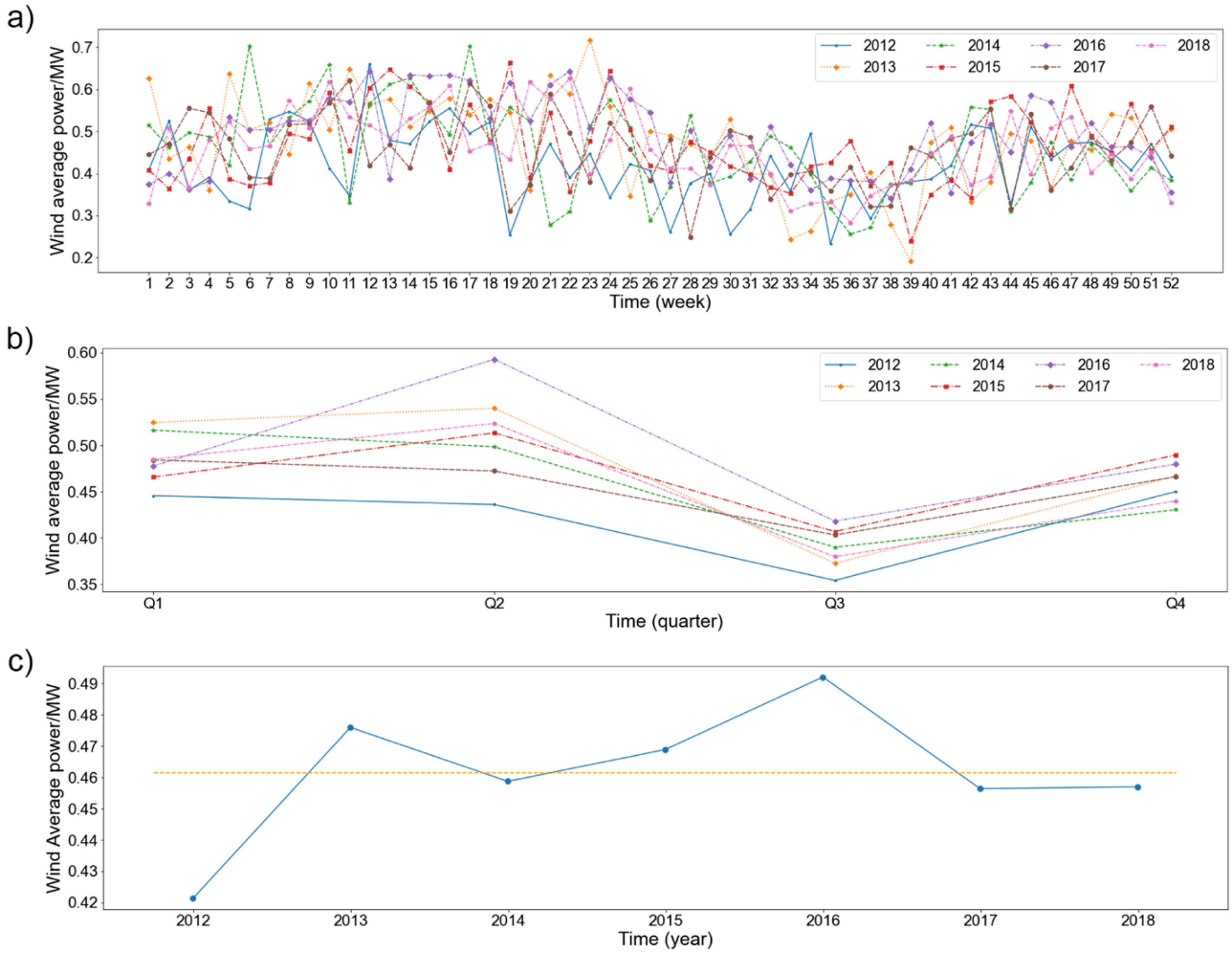

Fig. 1. Multi-timescale variability of renewable wind energy generation: (a) weekly, (b) seasonal, and (c) yearly.

2) Run the ESOM of interest on smaller period $T_i', i \in 1, 2, \ldots, m$ and extract features from the model like decision variables and dual variables;

3) On the basis of procedure 2), a mapping between period and extracted features is established. Perform an appropriate clustering algorithm on the features and obtain representative periods along with corresponding weights. The weights denote how many periods in the whole time horizon the selected periods represent;

4) Solve the ESOM on the representative periods selected.

In adaptive time aggregation, by implementing procedure 2), the ESOM defined on a small time slice is solved, and the model outcomes like decision variables could be accessed. Then, features containing both information from the ESOM and original input data variation along time could be extracted from the model outcomes for each time slice. In other words, the features are obtained through dimension reduction, using the ESOM as a non-linear transformer. These intrinsic features can be extracted from anywhere in the ESOM such as decision variables, dual variables, slack variables, etc., as long as they contribute to finding the best representative time slices to approximate the benchmark solution of the full time horizon. For CEMs, specifically, the features could be planned capacities or costs of each type of generation technology. From the ESOM defined before, five decision variables are selected: solar capacity, wind capacity, storage energy capacity, storage power capacity, and thermal generator capacity, the distribution of which are shown in Fig. 3. Typically, features for clustering should be normalized first to avoid the influence on final results brought by dimensions imbalance, the capacity features we use in this study have similar magnitude, so we kept the feature space free of normalization. Through the clustering on the feature space, time slices with similar capacity planning outcomes are clustered together and represented by one time slice. While our method provides a tool for more accurate evaluation of the future generation technology mix evolution/pathway, a more complicated empirical analysis is beyond the scope of the paper, as we are focused on presenting and validating the performance of our proposed method. To evaluate the approximation error of our method and existing methods, the model must be computationally tractable for the full time horizon without any approximation to generate benchmarks.

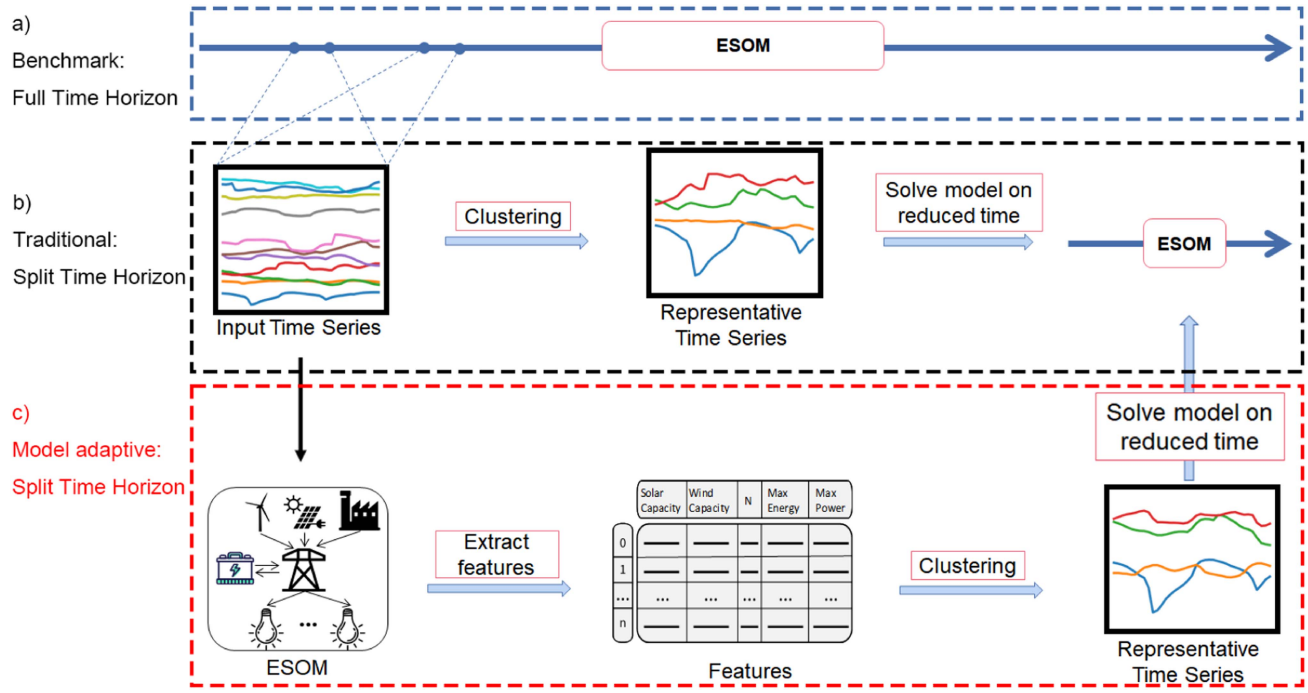

Fig. 2. Schematics of time aggregation: (a) benchmark: solving full time horizon model; (b) traditional time aggregation: clustering on raw data; (c) model adaptive time aggregation: clustering on features extracted from models.

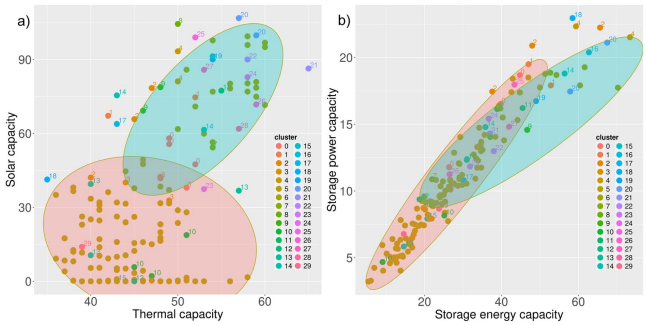

Fig. 3. Decision variable clustering from the full version Integer model of 30 representative weeks: (a) thermal & solar capacity (b) storage energy & power capacity. In the 30 clusters, two main clusters that contain the most time slices, indexed as 5 and 6, are highlighted with an epsilon border to show that these time slices are grouped together. The remaining clusters typically have no more than 2 time slices, which could be latent extreme periods.

Fig. 3 shows solar capacity, thermal capacity, storage power and energy capacity from the ESOM described in 1-17 with 30 representative weeks. On the basis of these extracted features, clustering algorithms could then be applied to find the most representative time slice.

To evaluate the performance of our proposed and traditional time aggregation methods in approximating the benchmark that solves the ESOM with the full time horizon [42], we use the metric of mean absolute percentage error (MAPE) in planning outcomes, defined as:

$$\text{MAPE} = \frac{1}{N}\sum_{i}^{N}\frac{|\hat{y}_i - y_i|}{y_i} \tag{18}$$

where y_i is the ith capacity planning outcome of the benchmark solution, and $\hat{y}_i$ is the ith capacity planning outcome estimated using a time aggregation method, either traditional or adaptive. MAPE estimates the average bias from needed capacity in benchmark, and the lower MAPE, the more accurate planning decisions that are required in future systems design can be calculated, and the more precise technology mix outcomes are obtained.

IV. Case Study

A. Case Setting

Two case studies are conducted to validate the method, one with a linear ESOM and the other with an integer one. Here capacities and profiles of wind, solar, and storage are considered as the aggregation of multiple units in an area. The capacities of renewable generation and storage and the number of thermal generation units are determined by the ESOM. The integer case is a full version of the ESOM presented in Section II in which only one type of thermal generation is used. In the linear case, thermal generation is removed from the portfolio, and the power demand is met by wind, solar, and energy storage systems only, which models a 100% renewable energy system. The integer variables for modelling the unit commitment of thermal generation units are therefore not needed. The solving process is fulfilled in a Linux-based server with two Intel Xeon E5-2680 v4 CPU clocking at 2.6 GHz and 756 GB of RAM by using commercial solver Gurobi. The codes for both cases are written in Python and could be found in [43].

The data used in the case study are from the supplementary information in [44], which contains 7 years data in hourly

TABLE I
OVERVIEW OF MODEL VARIABLES AND CONSTRAINTS

	Linear (7 years/30 representative weeks)			Integer (3 years/50 representative weeks)		
	Continuous	Integer	Constraints	Continuous	Integer	Constraints
Benchmark	306610	0	7×61320	131050	78625	14×26208
Traditional/ Cost Oriented/ Adaptive Time Aggregation	25210	0	7×5040	42010	25201	7×8400

[1] The numbers of continuous and integer variables are obtained from solving logs.
[2] The numbers of constraints are obtained by calculating the active constraints in the model. Due to the fact that constraints are indexed by time series, it's presented in the form of the number of constraints $\times$ the length of time series.

resolution of wind, solar and demand profiles from 2007 to 2013. The solar profiles are taken from the U.S. Energy Information Administration (EIA) Form 860 databases, and averaged for each region. And data on wind capacity factors is taken from NREL's Wind Integration National Dataset Toolkit (WIND Toolkit). Demand profiles are drawn from real demand data. The data sets are generated for each region, but here only part of Texas is used. To capture enough variability in a single representative period, here a week's data is bundled together as a time slice, which is 168 points at an hourly resolution. Many articles [45], [46] select representative days using clustering methods to ease computational burden with the planning horizon usually being no more than a year, which is far from requirements for data in long-term ESOMs, especially with renewable energy and storage systems. For the integer cases, the time horizon is reduced from 7 to 3 years, and MIP gap from 1e-4 to 1e-3, to keep the benchmark model solvable in a reasonable time frame. The overview of variable types and numbers in two version of models are shown in the Table I.

K-means and hierarchical clustering methods with different linkages are applied to compare how different clustering methods affect the accuracy of time aggregation. Basically, we use agglomerative clustering with single linkage [47] which is the shortest distance of each pair of different clusters for its outstanding performance. Agglomerative clustering is a hierarchical clustering technique which establishes a dendrogram for a data set on the basis of pre-defined distance measure of different groups. The clusters are obtained by cutting the dendrogram, and the results are stable across different runs of the algorithm.

In order to generate different ESOM settings, the renewable portfolio standard is varied from 50% to 95% in integer model, yielding 10 different policy constrained scenarios. For linear cases, different combinations of unit capacity costs are used to produce 16 different scenarios. The investment costs of solar, wind, battery power and energy are set to 50% and 150% of the cost values in Table II for different scenarios.

TABLE II
MAIN PARAMETERS IN THE ESOM

Model Parameters	Type	Value
Battery Energy	CAPEX	200 $/kWh
Battery Power	CAPEX	70 $/kW
Photovoltaic Panel	CAPEX	1000 $/kW
Wind Turbine	CAPEX	1500 $/kW
Thermal Plant	CAPEX	1000 $/kW
Battery Charing and Discharging	OPEX	50 $/MWh
Thermal Generation	OPEX	30 $/MWh
Up Time	Other	6 hrs
Down Time	Other	6 hrs

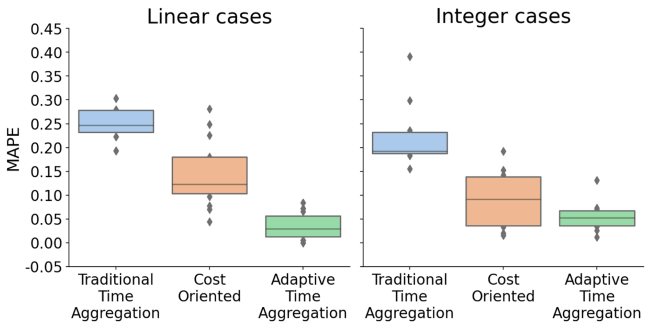

Fig. 4. MAPE of decision variables of traditional and adaptive time aggregation with linear and integer cases. In traditional time aggregation, representative periods are generated by clustering raw input. Adaptive time aggregation is the method we propose. Cost-oriented time aggregation is used to denote the method adopted in previous research [35] in which investment costs are used as features. To ensure the time length is the same, the representative periods in cost-oriented time aggregation are selected to be 210 and 350 days for linear and integer cases, while in our proposed method the time period is a week and the number of clusters are 30 and 50, respectively.

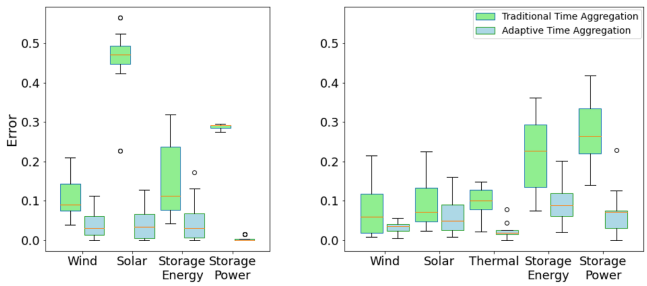

Fig. 5. Errors of decision variables of traditional and adaptive time aggregation with linear and integer cases. In linear cases, capacity of wind, solar, storage energy and storage power are decomposed to show errors of each term, while in integer cases, thermal capacity is further modeled and measured.

B. Performance of Adaptive Time Aggregation

In Fig. 4, the results of the linear cases show a 21.5% reduction in MAPE using our proposed adaptive time aggregation method compared to the traditional one. The MAPE of the adaptive method can be as low as 3.5% in linear cases. In the integer cases, the adaptive time aggregation method also brings a 16.9% decrease in MAPE compared to traditional one. Compared to existing similar works [35] in which investment cost terms are used as features, our features yielded a 10.7% and 3.62% reduction in MAPE for linear and integer models, respectively. Besides the reduction, it could be seen that our adaptive time aggregation method has lower deviation and more stable performance than both traditional and cost-oriented methods. In Fig. 5, the adaptive method has lower errors for each of the capacity decision variables. It performs better in capturing IRE's characteristics given that in both linear and integer cases the

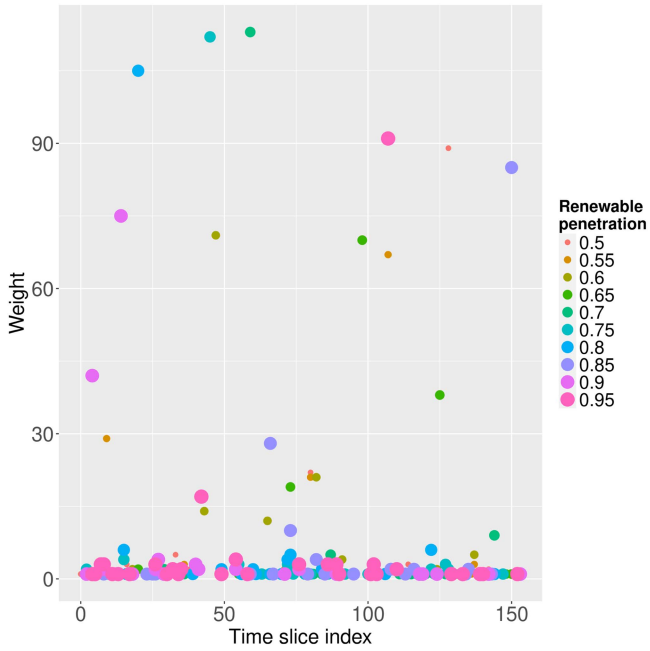

Fig. 6. Selected time periods and weights with varying renewable portfolio standards.

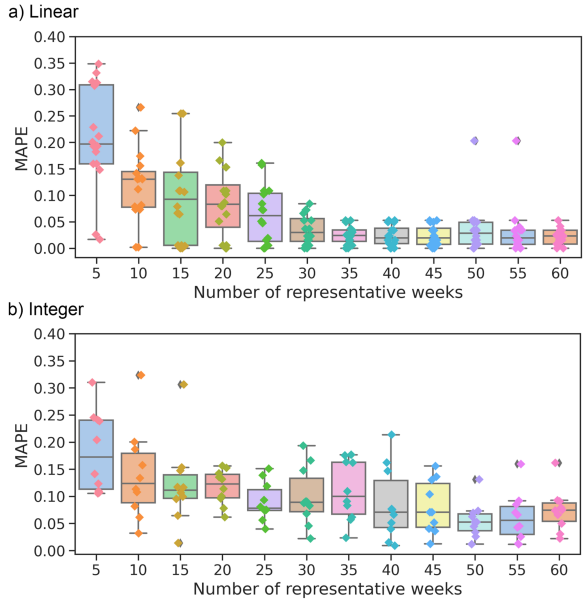

Fig. 7. MAPE with different clustering numbers: (a) Linear cases (b) Integer cases.

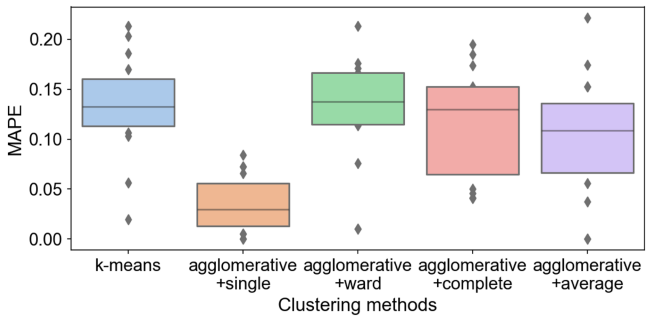

Fig. 8. MAPE with different clustering methods.

errors on capacity of wind and solar are on average lower than half of those in traditional time aggregation method.

In terms of solving efficiency, linear and integer cases take 335 seconds and 2 hours in solving benchmark models, respectively. While using model-adaptive time aggregation method, it takes about 244 seconds to train and obtain representative weeks for linear cases and 245 seconds for integer ones. Considering that only three years of data are used in integer cases, it might be scaled to 572 seconds to train a seven-year case of integer model. The elapsed time for solving the model is shortened to 10 seconds in linear cases and 89 seconds in integer ones. Our proposed method could remarkably reduce the total computational time to less than five minutes, eliminating much computational burden, especially for MILP.

Why is our proposed adaptive method effective? Intuitively, our adaptive time aggregation method process embeds similarity information from the ESOM's perspective, and thus the selected time periods have greater power in representing the whole time horizon. Fig. 6 shows how the representative period selection is adaptive to different model policy settings. If the weight is 0, then this time slice is not selected and is represented by another slice. If the weight is positive, this time slice is selected and represents some slices after clustering. Different colors represent the weights with different renewable portfolio policies, from 50% to 95%. The system setting changes when the renewable penetration changes. As shown in Fig. 6, when the system changes, the clustering results change as well. For example, with 85% renewable penetration, the week with the highest weight is the week number 150, while with 80% renewable penetration, the week with the highest weight is the week number 20. This indicates that our clustering results is adaptive to the change in ESOM.

C. *Appropriate Number of Representative Time Periods*

Generally we regard that to some extent, there exists a certain number of representative time periods that include enough information to approximate the full time horizon with limited errors. So with the number of clusters getting close to this level, the MAPE should drop to an appropriate level and the results will be more acceptable. In [48], Elbow's rule [49] is adopted to select an appropriate clustering number for picking representative periods to solve a transmission expansion planning, and a lower operating cost error below 3% is obtained. There are many other criteria to select an appropriate clustering number [49]. Fig. 7 shows the approximation errors of adaptive time aggregation with different numbers of clusters in linear and integer cases. We searched a clustering number space from 5 to 60, stepped by 5. Fig. 7(a) shows the trend in linear cases, when the number of clusters reaches 30, the MAPE decreases slowly as the number of clusters increases. The situation is similar in Fig. 7(b) for integer cases that MAPE decreases when number of clusters increases and 50 representative weeks yields a relatively low MAPE of 5.56%.

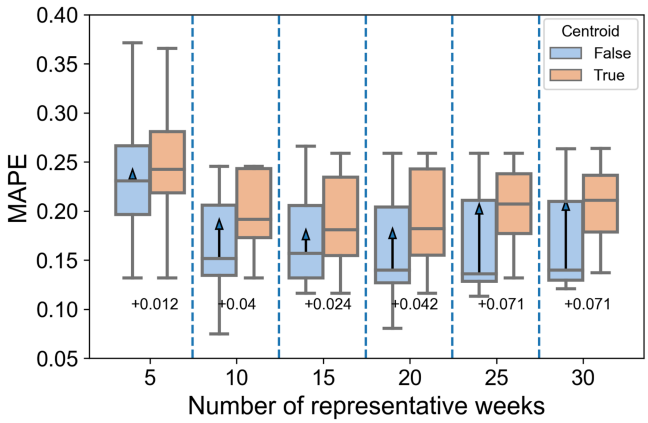

Fig. 9. MAPE with different centroid setting.

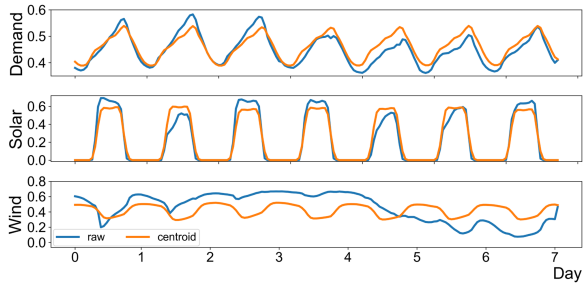

Fig. 10. Representative week data of wind & solar power and load curve.

Different clustering methods perform diversely in MAPE, among which agglomerative clustering with single linkage has an average error of 3.5%. Other methods like K-means, which is often used in representative time period selection, and other linkage modes yield errors with a mean between 10% and 15%. Although agglomerative clustering with average linkage sometimes can yield a lower error, its mean performance is worse than that with single linkage. These results justify our clustering setting for the base case.

D. The Smoothing Effect of Cluster Centroid

After clustering, either the centroid points or the time slices closest to the centroids of each cluster can be used as the representative periods, with the number of slices in that cluster assigned as corresponding weights [42], [50]. Here we examine two settings: using the centroid (centroid option True) and using the time slice closest to the centroid (centroid option False). As shown in Fig. 9, using the centroid increases the approximation error for all numbers of clusters. Mathematically, using the centroid means that the variation in the same cluster is averaged by other points. As shown in Fig. 10, the centroid point usually represents smoother profiles of wind, solar, and load, and those extreme values in the raw profiles will be lost if the centroid is used as the representative point. For example, the raw wind power data of the week closest to the centroid has a larger variation than the profile of the centroid, and the centroid profile gets smoother and more periodic after averaging. In ESOMs, the capacity expansion decisions are not only dependent on typical days/weeks but also extreme days/weeks [51], and may be even more sensitive to the extreme scenarios which challenge the reliability of energy systems. Across representative periods, common and rare events are both appropriately selected and weighted through the clustering method, but within representative periods, averaged data can still smooth the variation especially in IRE, resulting in underestimation of required capacities like the wind power and storage capacities.

V. Conclusion

In this article we proposed a model-adaptive clustering-based time aggregation method to better select representative periods for solving long-term ESOMs. New features are extracted based on ESOMs to improve approximation performance over traditional time aggregation which have great potential to be used in energy system capacity planning problems [32] and economic dispatch problems [29]. Two versions of an ESOM are designed to validate the proposed method, and the results show that the method can sufficiently reduce the approximation errors, compared to traditional time aggregation, while keeping the ESOM tractable. On the basis of clustering methods, deeper exploration into feature extraction and method settings are made to best exploit the performance of the proposed method.

By implementing this model-adaptive time aggregation method, the features from ESOMs are linked to each time period, allowing for a representation with lower dimensions. These features do help capture the characteristics of both variability in renewable sources and ESOMs. Only decision variables are used in the method validation, but there are lots of other features like dual variables of the ESOM. Exploring more relevant features from ESOMs is an interesting direction of future study.

References

[1] V. Masson-Delmotte et al., "Global warming of 1.5°C. An IPCC Special Report on the impacts of global warming of 1.5°C above pre-industrial levels and related global greenhouse gas emission pathways, in the context of strengthening the global response to the threat of climate change, sustainable development, and efforts to eradicate poverty," Dec. 2018, doi: 10.1017/9781009157940.

[2] M. Da Graça Carvalho, "Eu energy and climate change strategy," *Energy*, vol. 40, no. 1, pp. 19–22, 2012.

[3] M. Davidson, V. J. Karplus, D. Zhang, and X. Zhang, "Policies and institutions to support carbon neutrality in China by 2060," *Econ. Energy Environ. Policy*, vol. 10, no. 2, pp. 7–25, 2021.

[4] *FACT SHEET: President biden sets 2030 greenhouse gas pollution reduction target aimed at creating good-paying union jobs and securing U.S. leadership on clean energy technologies*, 2021. [Online]. Available: https://www.whitehouse.gov/briefing-room/statements-releases/2021/04/22/fact-sheet-president-biden-sets-2030-greenhouse-gas-pollution-reduction-target-aimed-at-creating-good-paying-union-jobs-and-securing-u-s-leadership-on-clean-energy-technologies

[5] A. Marcucci, S. Kypreos, and E. Panos, "The road to achieving the long-term paris targets: Energy transition and the role of direct air capture," *Climatic Change*, vol. 144, no. 2, pp. 181–193, 2017.

[6] S. M. Wheeler, "A carbon-neutral california: Social ecology and prospects for 2050 GHG reduction," *Urban Plan.*, vol. 2, no. 4, pp. 5–18, 2017.

[7] N. L. Panwar, S. C. Kaushik, and S. Kothari, "Role of renewable energy sources in environmental protection: A review," *Renewable Sustain. Energy Rev.*, vol. 15, no. 3, pp. 1513–1524, 2011.

[8] U. IEA, "Global energy review 2020," Accessed: 10 Sep. 2020, 2020. [Online]. Available: https://www.iea.org/countries/

[9] I. B. Fridleifsson, "Geothermal energy for the benefit of the people," *Renewable Sustain. Energy Rev.*, vol. 5, no. 3, pp. 299–312, 2001.

[10] R. Bessa, C. Moreira, B. Silva, and M. Matos, "Handling renewable energy variability and uncertainty in power systems operation," *Wiley Interdiscipl. Reviews: Energy Environ.*, vol. 3, no. 2, pp. 156–178, 2014.

[11] R. Golden and B. Paulos, "Curtailment of renewable energy in california and beyond," *Electricity J.*, vol. 28, no. 6, pp. 36–50, 2015.

[12] P. Denholm, M. O'Connell, G. Brinkman, and J. Jorgenson, "Overgeneration from solar energy in california. a field guide to the duck chart," *Nat. Renewable Energy Lab.*, Golden, CO, USA, Tech. Rep. NREL/TP-6A20-65023, 2015.

[13] S. Koohi-Fayegh and M. Rosen, "A review of energy storage types, applications and recent developments," *J. Energy Storage*, vol. 27, 2020, Art. no. 101047.

[14] A. Oudalov, R. Cherkaoui, and A. Beguin, "Sizing and optimal operation of battery energy storage system for peak shaving application," in *Proc. IEEE Lausanne Power Tech.*, 2007, pp. 621–625.

[15] D.-I. Stroe, V. Knap, M. Swierczynski, A.-I. Stroe, and R. Teodorescu, "Operation of a grid-connected lithium-ion battery energy storage system for primary frequency regulation: A battery lifetime perspective," *IEEE Trans. Ind. Appl.*, vol. 53, no. 1, pp. 430–438, Jan./Feb. 2017.

[16] Y. Zhu, C. Liu, K. Sun, D. Shi, and Z. Wang, "Optimization of battery energy storage to improve power system oscillation damping," *IEEE Trans. Sustain. Energy*, vol. 10, no. 3, pp. 1015–1024, Jul. 2019.

[17] P. F. Ribeiro, B. K. Johnson, M. L. Crow, A. Arsoy, and Y. Liu, "Energy storage systems for advanced power applications," *Proc. IEEE Proc. IRE*, vol. 89, no. 12, pp. 1744–1756, Dec. 2001.

[18] P. Ralon, M. Taylor, A. Ilas, H. Diaz-Bone, and K. Kairies, "Electricity storage and renewables: Costs and markets to 2030," Int. Renewable Energy Agency, Abu Dhabi, UAE, vol. 164, 2017.

[19] B. Alizadeh and S. Jadid, "Reliability constrained coordination of generation and transmission expansion planning in power systems using mixed integer programming," *IET Gener. Transmiss. Distrib.*, vol. 5, no. 9, pp. 948–960, 2011.

[20] H. Haghighat and B. Zeng, "Bilevel mixed integer transmission expansion planning," *IEEE Trans. Power Syst.*, vol. 33, no. 6, pp. 7309–7312, Nov. 2018.

[21] A. Khodaei, M. Shahidehpour, L. Wu, and Z. Li, "Coordination of short-term operation constraints in multi-area expansion planning," *IEEE Trans. Power Syst.*, vol. 27, no. 4, pp. 2242–2250, Nov. 2012.

[22] P. M. Castro, I. E. Grossmann, and Q. Zhang, "Expanding scope and computational challenges in process scheduling," *Comput. Chem. Eng.*, vol. 114, pp. 14–42, 2018.

[23] V. Oree, S. Z. Sayed Hassen, and P. J. Fleming, "Generation expansion planning optimisation with renewable energy integration: A review," *Renewable Sustain. Energy Rev.*, vol. 69, pp. 790–803, 2017.

[24] H. Teichgraeber et al., "Extreme events in time series aggregation: A case study for optimal residential energy supply systems," *Appl. Energy*, vol. 275, 2020, Art. no. 115223.

[25] X. Zhang and D. J. Hil, "Hierarchical temporal and spatial clustering of uncertain and time-varying load models," 2020, doi: 10.48550/ARXIV.2006.16493.

[26] G. Haydt, V. Leal, A. Pina, and C. A. Silva, "The relevance of the energy resource dynamics in the mid/long-term energy planning models," *Renewable Energy*, vol. 36, no. 11, pp. 3068–3074, 2011.

[27] K. Poncelet, "Long-term energy-system optimization models—capturing the challenges of integrating intermittent renewable energy sources and assessing the suitability for descriptive scenario analyses," 2018. [Online]. Available: https://lirias.kuleuven.be/1745696?limo=0

[28] A. Pina, C. A. Silva, and P. Ferrão, "High-resolution modeling framework for planning electricity systems with high penetration of renewables," *Appl. Energy*, vol. 112, pp. 215–223, 2013.

[29] M. Welsch et al., "Supporting security and adequacy in future energy systems: The need to enhance long-term energy system models to better treat issues related to variability," *Int. J. Energy Res.*, vol. 39, no. 3, pp. 377–396, 2015.

[30] P. Nahmmacher, E. Schmid, L. Hirth, and B. Knopf, "Carpe diem: A novel approach to select representative days for long-term power system modeling," *Energy*, vol. 112, pp. 430–442, 2016.

[31] M. Zatti et al., "k-MILP: A novel clustering approach to select typical and extreme days for multi-energy systems design optimization," *Energy*, vol. 181, pp. 1051–1063, 2019.

[32] R. Domínguez and S. Vitali, "Multi-chronological hierarchical clustering to solve capacity expansion problems with renewable sources," *Energy*, vol. 227, 2021, Art. no. 120491.

[33] S. Pfenninger, "Dealing with multiple decades of hourly wind and PV time series in energy models: A comparison of methods to reduce time resolution and the planning implications of inter-annual variability," *Appl. Energy*, vol. 197, pp. 1–13, 2017.

[34] H. Teichgraeber, L. E. Küpper, and A. R. Brandt, "Designing reliable future energy systems by iteratively including extreme periods in time-series aggregation," *Appl. Energy*, vol. 304, 2021, Art. no. 117696.

[35] M. Sun, F. Teng, X. Zhang, G. Strbac, and D. Pudjianto, "Data-driven representative day selection for investment decisions: A cost-oriented approach," *IEEE Trans. Power Syst.*, vol. 34, no. 4, pp. 2925–2936, Jul. 2019.

[36] A. P. Hilbers, D. J. Brayshaw, and A. Gandy, "Importance subsampling: Improving power system planning under climate-based uncertainty," *Appl. Energy*, vol. 251, 2019, Art. no. 113114.

[37] K. Poncelet, H. Höschle, E. Delarue, A. Virag, and W. D'haeseleer, "Selecting representative days for capturing the implications of integrating intermittent renewables in generation expansion planning problems," *IEEE Trans. Power Syst.*, vol. 32, no. 3, pp. 1936–1948, May 2017.

[38] T. Mertens, K. Bruninx, J. Duerinck, and E. Delarue, "Adequacy aware long-term energy-system optimization models considering stochastic peak demand," *Adv. Appl. Energy*, vol. 4, 2021, Art. no. 100072.

[39] K. Poncelet, E. Delarue, and W. D'haeseleer, "Unit commitment constraints in long-term planning models: Relevance, pitfalls and the role of assumptions on flexibility," *Appl. Energy*, vol. 258, 2020, Art. no. 113843.

[40] B. S. Palmintier and M. D. Webster, "Heterogeneous unit clustering for efficient operational flexibility modeling," *IEEE Trans. Power Syst.*, vol. 29, no. 3, pp. 1089–1098, May 2014.

[41] W. W. Tso, C. D. Demirhan, C. F. Heuberger, J. B. Powell, and E. N. Pistikopoulos, "A hierarchical clustering decomposition algorithm for optimizing renewable power systems with storage," *Appl. Energy*, vol. 270, 2020, Art. no. 115190.

[42] L. Reichenberg, A. S. Siddiqui, and S. Wogrin, "Policy implications of downscaling the time dimension in power system planning models to represent variability in renewable output," *Energy*, vol. 159, pp. 870–877, 2018.

[43] Y. Zhang and G. He, "Adaptive-clustering-for-ESOM," version 1.0.0, 2021, doi: 10.5281/zenodo.1234. [Online]. Available: https://github.com/Betristor/Adaptive-clustering-for-ESOM

[44] N. A. Sepulveda, J. D. Jenkins, A. Edington, D. S. Mallapragada, and R. K. Lester, "The design space for long-duration energy storage in decarbonized power systems," *Nature Energy*, vol. 6, no. 5, pp. 506–516, 2021.

[45] A. García-Cerezo, L. Baringo, and R. García-Bertrand, "Representative days for expansion decisions in power systems," *Energies*, vol. 13, no. 2, 2020, Art. no. 335.

[46] M. Gamst, S. Buchholz, and D. Pisinger, "Time aggregation techniques applied to a capacity expansion model for real-life sector coupled energy systems," 2020, *arXiv:2012.10244*.

[47] T. Hastie, R. Tibshirani, J. H. Friedman, and J. H. Friedman, *The Elements of Statistical Learning: Data Mining, Inference, and Prediction*, vol. 2, Berlin, Germany: Springer, 2009.

[48] N. González-Cabrera, J. Ortiz-Bejar, A. Zamora-Mendez, and M. R. Arrieta Paternina, "On the improvement of representative demand curves via a hierarchical agglomerative clustering for power transmission network investment," *Energy*, vol. 222, 2021, Art. no. 119989.

[49] T. M. Kodinariya and P. R. Makwana, "Review on determining number of cluster in k-means clustering," *Int. J.*, vol. 1, no. 6, pp. 90–95, 2013.

[50] I. J. Scott, P. M. Carvalho, A. Botterud, and C. A. Silva, "Clustering representative days for power systems generation expansion planning: Capturing the effects of variable renewables and energy storage," *Appl. Energy*, vol. 253, 2019, Art. no. 113603.

[51] D. Young et al., "Program on technology innovation: US-REGEN model documentation," EPRI, Palo Alto, CA, USA, 2014.